

Supporting Information

High-Density Platinum Nanoparticle-Decorated Titanium Dioxide Nanofiber Network for Efficient Capillary Photocatalytic Hydrogen Generation

Zhaodong Li,^a Chunhua Yao,^a Yi-Cheng Wang,^b Solomon Mikael,^c Sundaram

Gunasekaran,^b Zhenqiang Ma,^c Zhiyong Cai,^{d,} Xudong Wang^{a,*}*

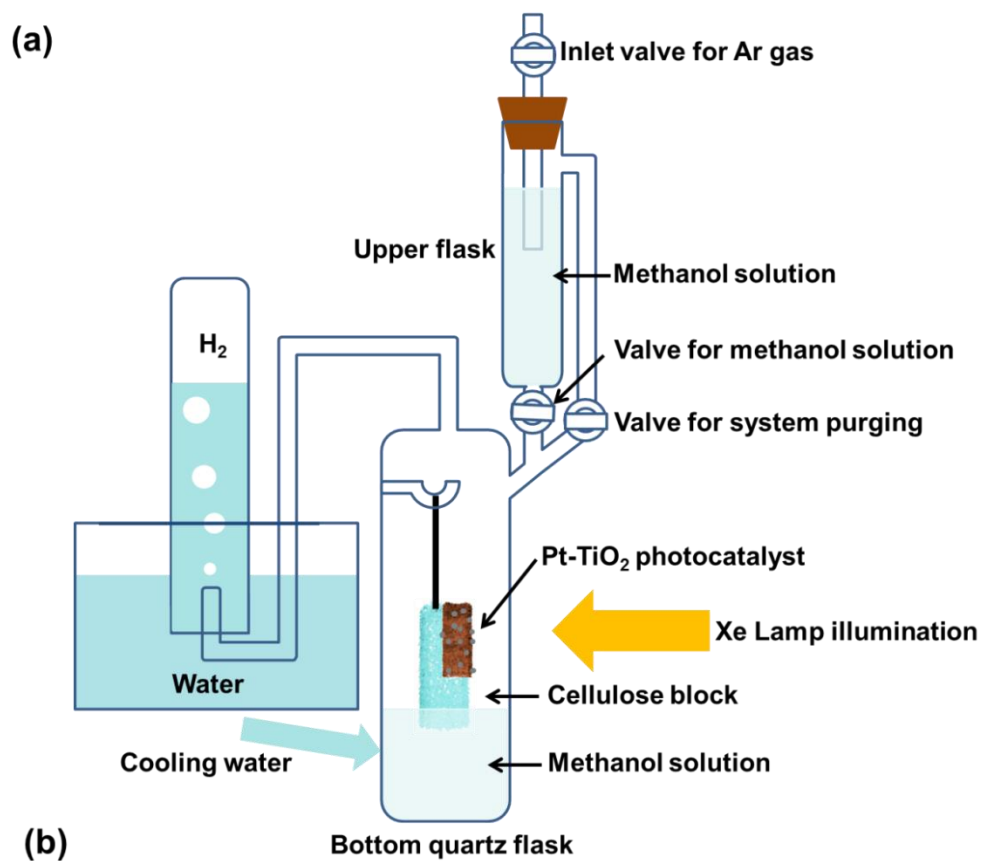
^aDepartment of Materials Science and Engineering, University of Wisconsin-Madison, Madison, WI 53706, USA

^bDepartment of Biological Systems Engineering, University of Wisconsin-Madison, Madison, WI 53706, USA

^cDepartment of Electrical and Computer Engineering, University of Wisconsin-Madison, Madison, WI 53706, USA

^dForest Products Laboratory, USDA Forest Service, Madison, WI 53726, USA

* **Email:** XW: xudong.wang@wisc.edu; ZC: zcai@fs.fed.us



(b)

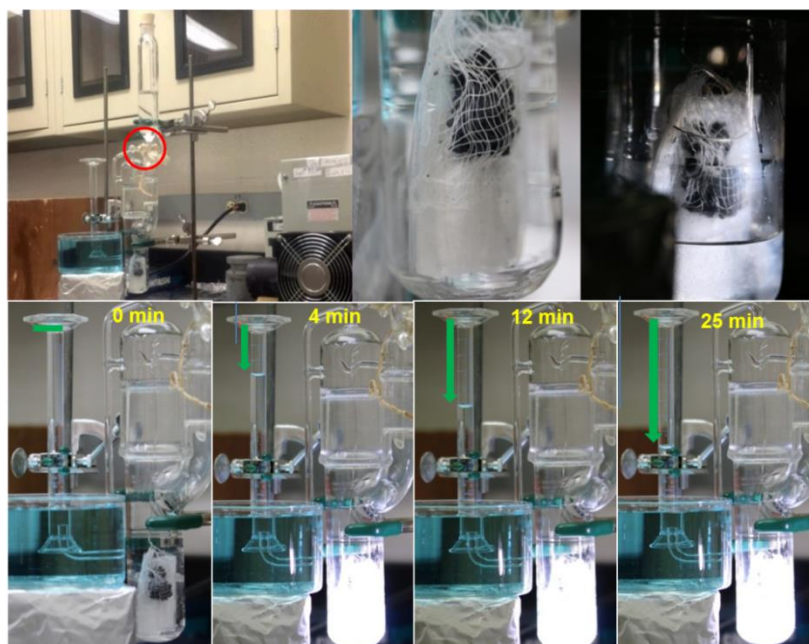


Figure S1. Schematics (a) and pictures (b) of typical apparatus configuration for H₂ production and collection when the whole Pt-TiO₂ composite-CNF was exposed under Xe lamp illumination. H₂ is evolved and collected as indicated by the green arrows.

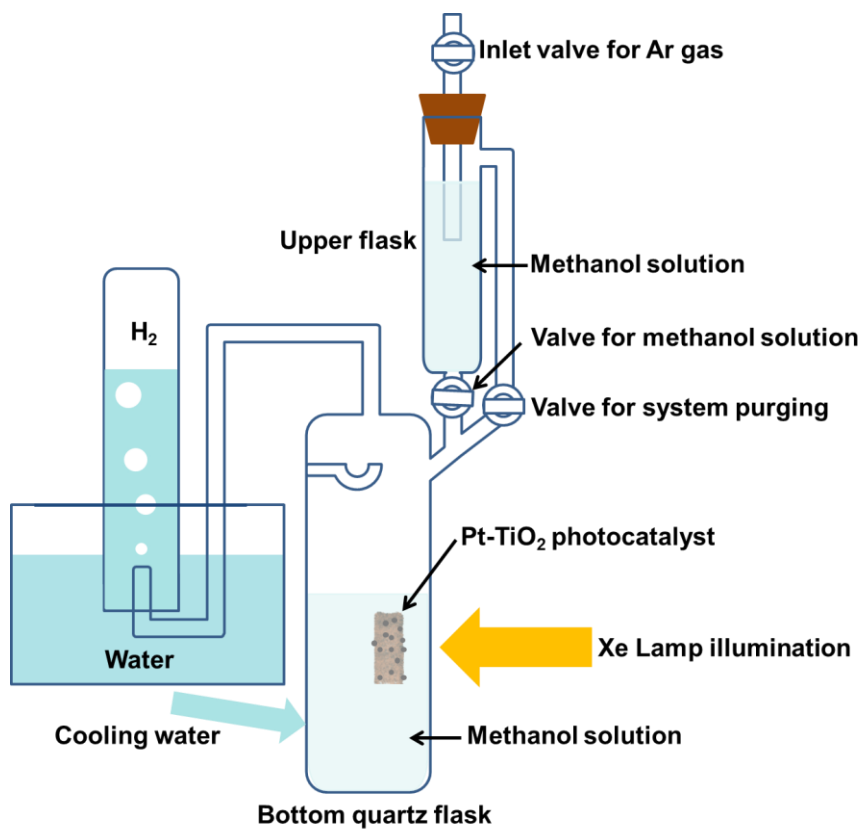


Figure S2. Schematics of conventional in-electrolyte reaction setup for H₂ production.

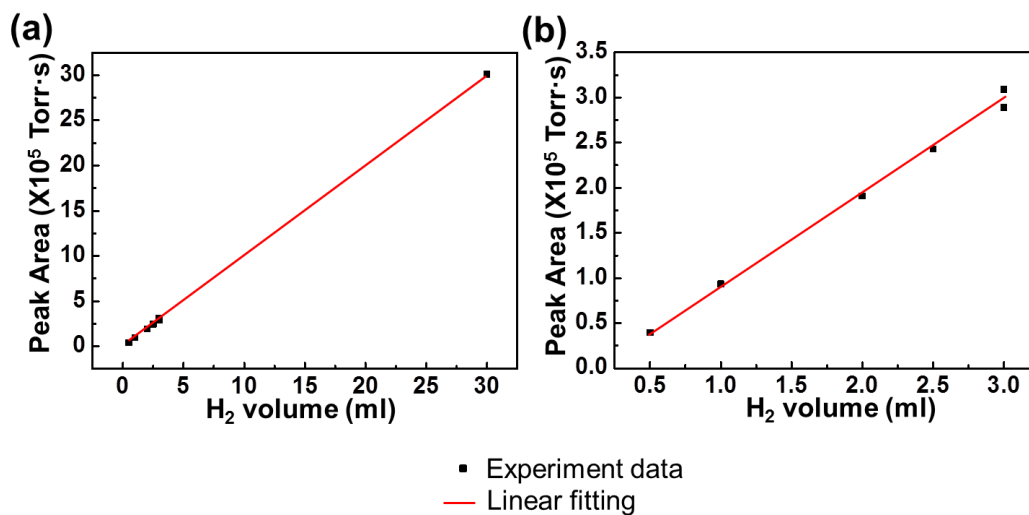


Figure S3. (a) The calibration curve of the Residue Gas Analyzer to determine the amount of H₂ by using standard H₂ in certain volumes (0.5, 1, 2, 2.5, 3, and 30 mL). (b) Zoom in view of the calibration curve using the standard H₂ ranging from 0.5 mL to 3 mL.

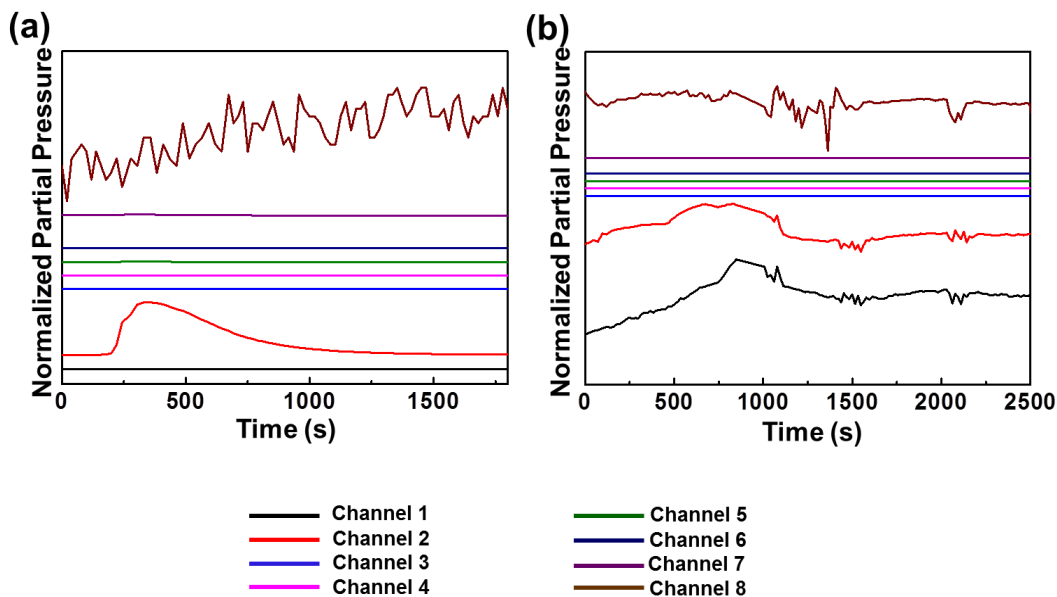


Figure S4. Normalized partial pressure of each setting channel versus measurement time by Residue Gas Analyzer. Every channel was set to detect the gas molecule with certain mass. (a) Result of the 30 mL H₂ sample, which is for calibration. (b) Result of the experiment gas sample, which was obtained from the 3 min capillary photocatalytic reaction at the beginning of sample T1. Since Ar may be contained in the gas sample as well as it was used as carrier gas during the RGA measurement, the obvious curve variation of channel 8 for Ar can be observed.

Table S1. Residue Gas Analyzer Measurement Channel List

No. of Channel	1	2	3	4	5	6	7	8
Detected Mass	1	2	3	16	18	28	32	40
Related ion/Molecule	H ⁺	H ₂	H ₃ ⁺	O ⁻	H ₂ O	Air	O ₂	Ar

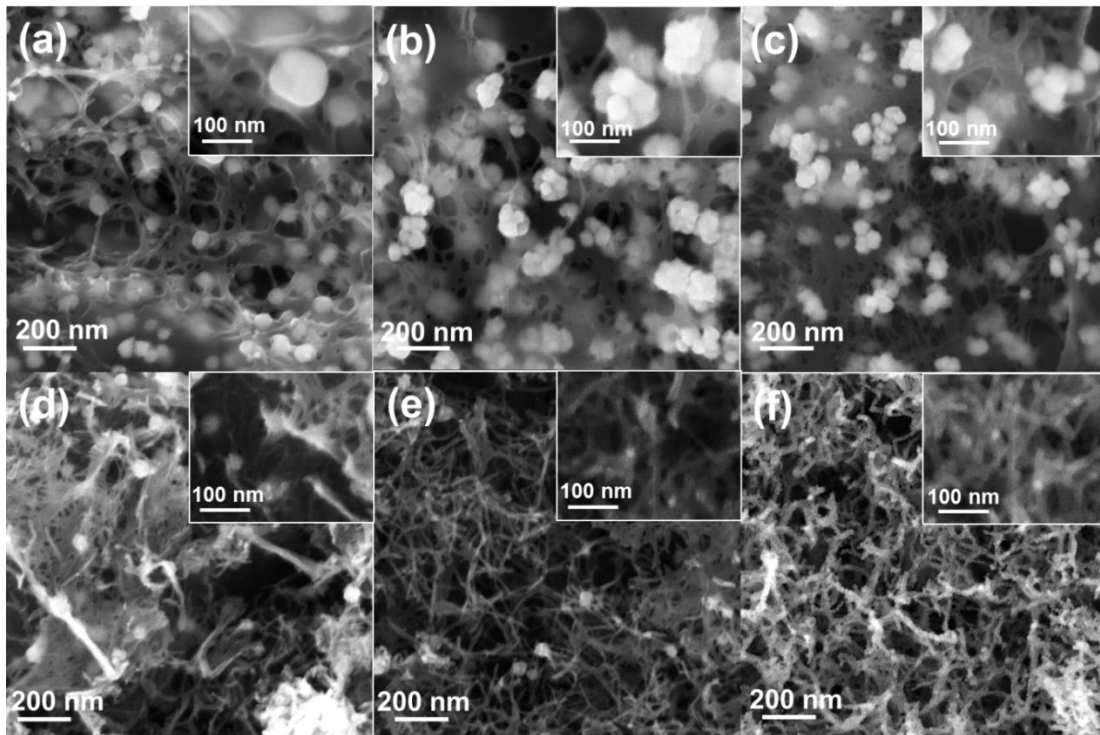


Figure S5. SEM images for the morphology comparison of three as-prepared Pt-CNFs templates and corresponding 3D fibrous Pt-TiO₂ composite samples.

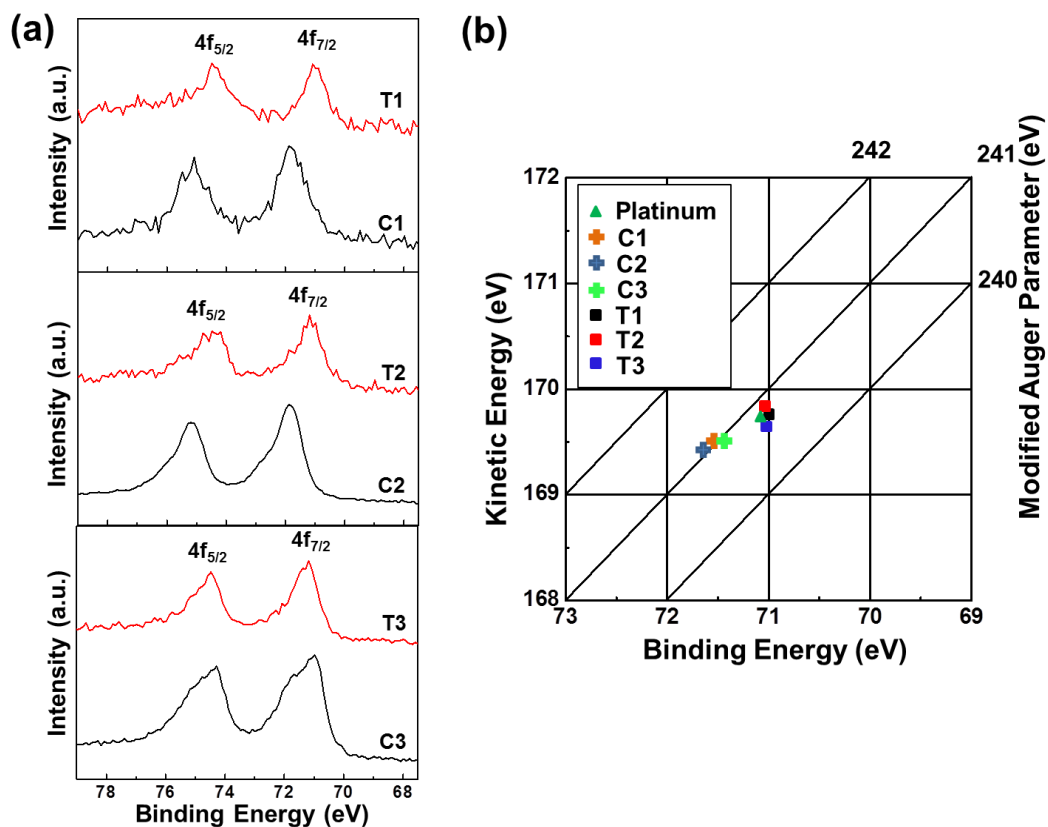


Figure S6. (a) Pt 4f XPS spectra for all three Pt-CNFs samples and their corresponding Pt-TiO₂ samples. (b) Wagner plot showing the modified auger parameters of Pt in all Pt-CNFs and their corresponding Pt-TiO₂ samples. The Pt chemical states in Pt-TiO₂ composites lie almost at the same position of metallic Pt (green triangle).

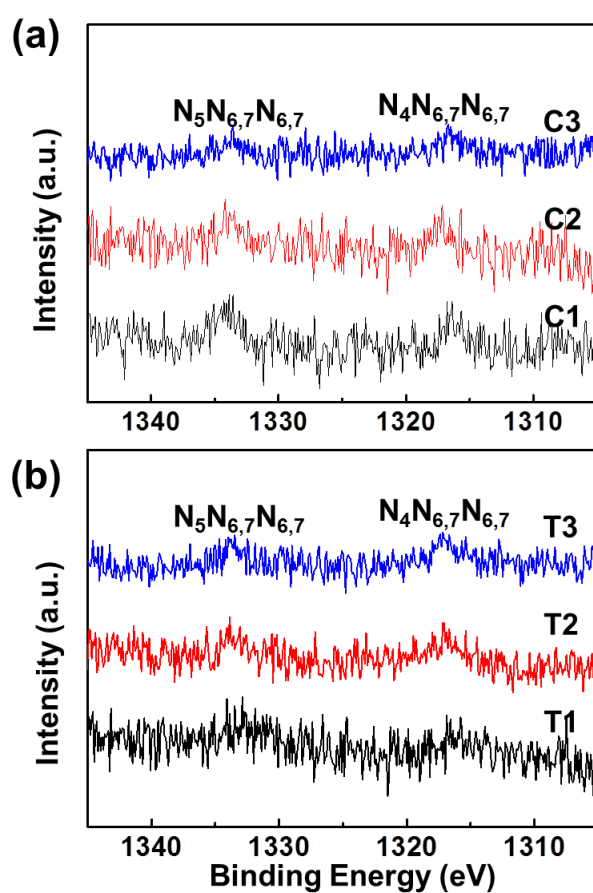


Figure S7. Pt auger spectra ($N_4N_{6,7}N_{6,7}$ and $N_5N_{6,7}N_{6,7}$) by XPS investigation for three Pt-CNFs templates (a) and corresponding 3D fibrous Pt-TiO₂ composite samples (b).

Wagner Plot

The modified auger parameter of Pt (the sum of kinetic energy of the Auger transition $N_4N_{6,7}N_{6,7}$ and Pt4f 7/2 binding energy) was used to plot the Wagner plot (chemical state plot) as shown in Figure S2. The Al K α X-ray photon energy (1486.6 eV) that we used in our experiment was used to obtain the kinetic energy of the Pt Auger transition $N_4N_{6,7}N_{6,7}$ (photon energy subtracted by the binding energy of Pt Auger transition $N_4N_{6,7}N_{6,7}$ in Figure S7).

In the Wagner plot, the Auger kinetic energy is on the ordinate, and the photoelectron binding energy is on the abscissa oriented in the negative direction. The modified Auger parameters are shown in the diagonal line. The Standard modified Auger parameters of metallic Pt were retrieved from the previous published works^{1,2} and plotted with the green triangle.

Reference

1. Powell, C. J. (2012). Recommended Auger parameters for 42 elemental solids. *Journal of Electron Spectroscopy and Related Phenomena*, 185(1), 1-3.
2. Powell, C. J. (2010). Recommended Auger-electron kinetic energies for 42 elemental solids. *Journal of Electron Spectroscopy and Related Phenomena*, 182(1), 11-18.

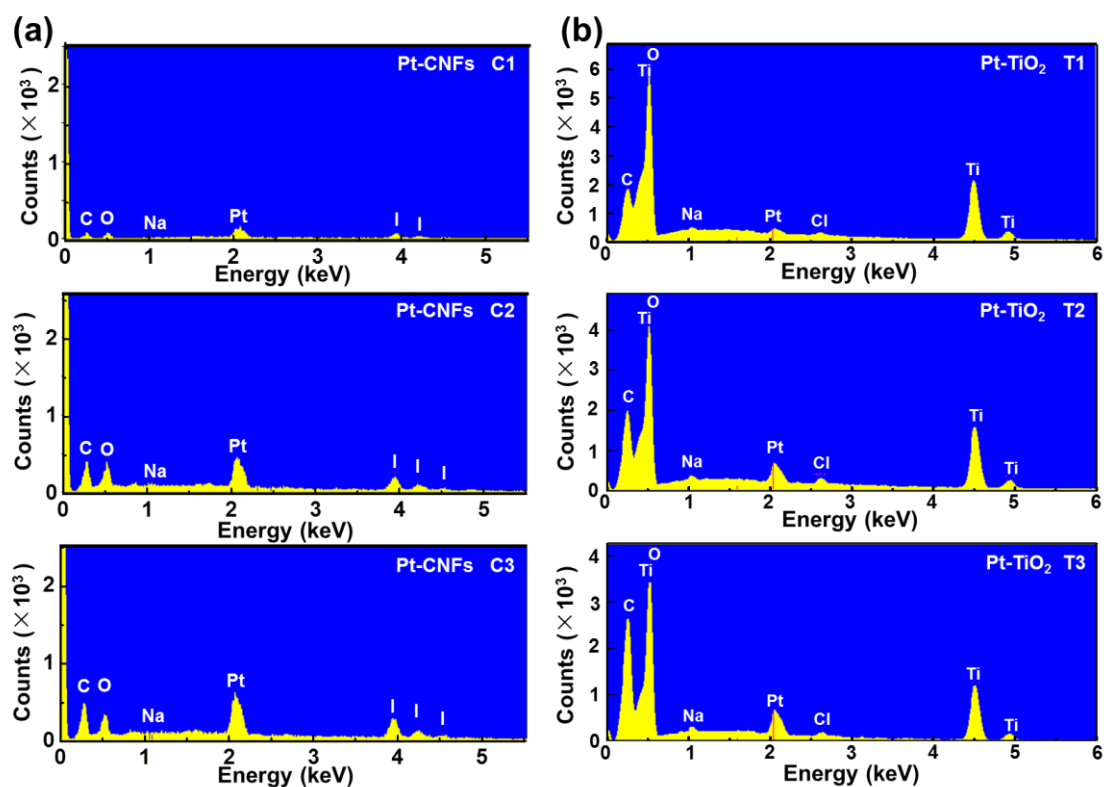


Figure S8. Energy-dispersive X-ray spectroscopy (EDS) for all three 3D (a) Pt-CNFs templates (C1, C2, and C3) and (b) Pt-TiO₂ composites (T1, T2, and T3).

Table S2. Pt weight ratios in three 3D Pt-CNFs templates from EDS characterizations and Pt weight ratios in three 3D Pt-TiO₂ composites from both EDS and ICP characterizations.

Pt-CNFs templates	Pt-TiO ₂ composites	
	EDS wt %	ICP wt %
C1	20.20	2.30
C2	33.26	7.72
C3	57.77	11.05

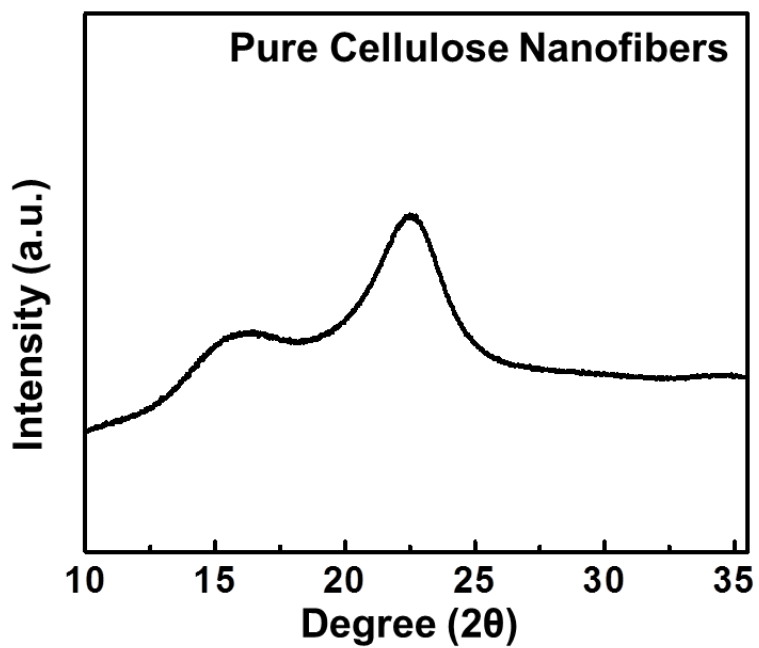


Figure S9. XRD of pure cellulose nanofibers (CNFs).

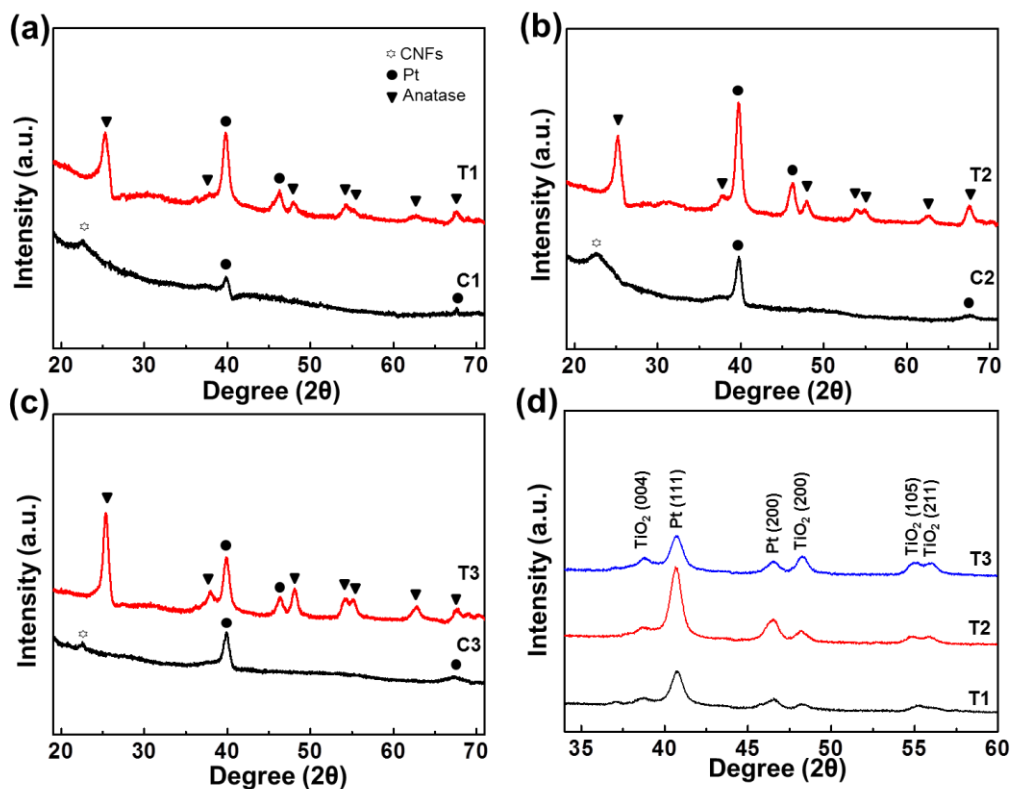


Figure S10. XRD carried on all three as-prepared Pt-CNFs templates (C1, C2, and C3) and 3D Pt-TiO₂ composites (T1, T2, and T3). (a-c) The cellulose diffraction peak at 23° can be only observed on Pt-CNFs templates. (d) The Pt diffraction peaks and anatase TiO₂ peaks are obtained on all Pt-TiO₂ samples.

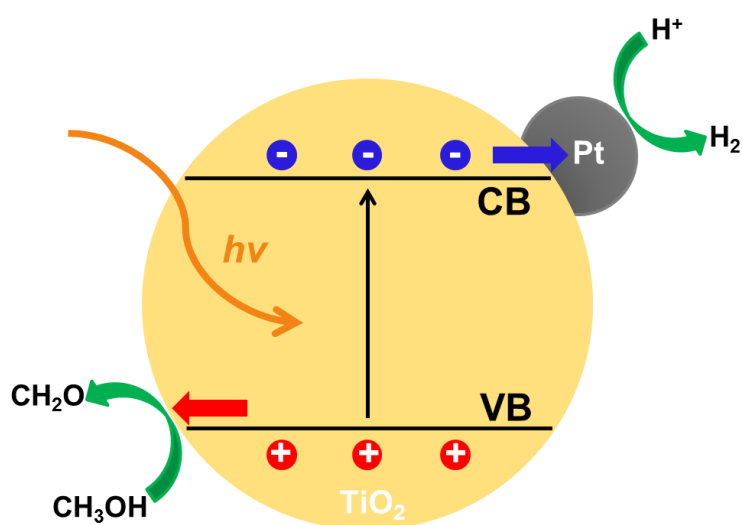


Figure S11. A Possible Reaction Mechanism for Photocatalytic H₂ generation in methanol aqueous solution

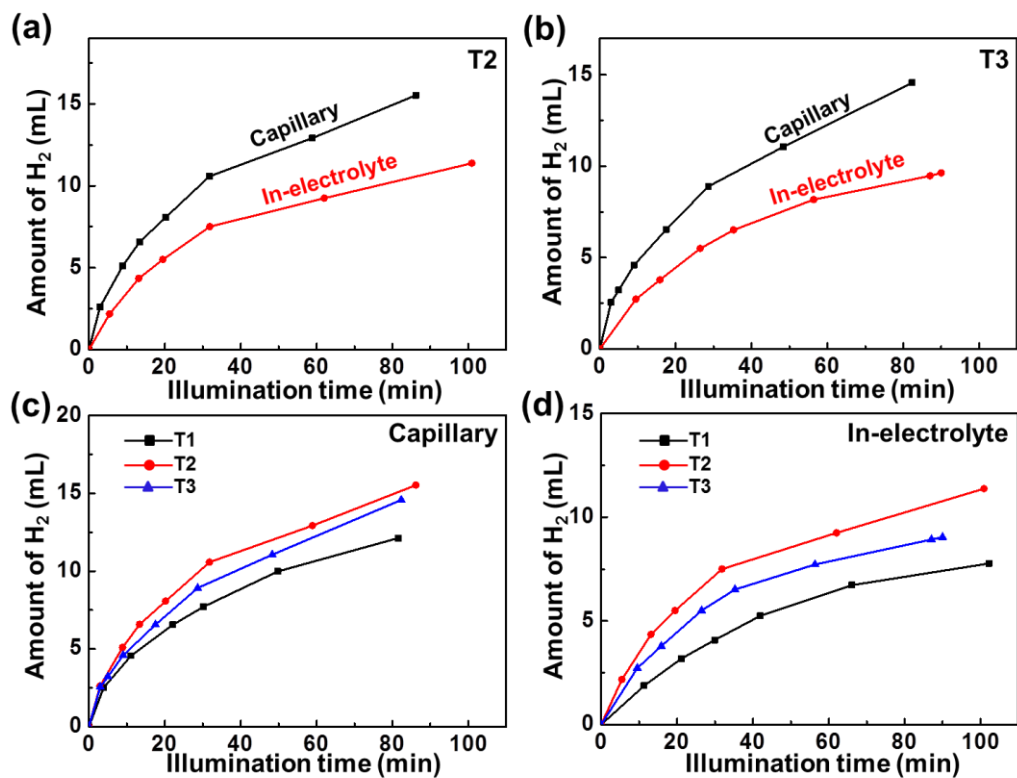


Figure S12. H₂ yield of Pt-TiO₂ in capillary setup and in-electrolyte setup from photocatalyst (a) T2 and (b) T3. (c,d) The comparison of H₂ amount from three 3D Pt-TiO₂ composites (T1, T2, and T3). In both capillary (c) and in-electrolyte setup (d), T3 photocatalyst exhibits the best ability on H₂ production.

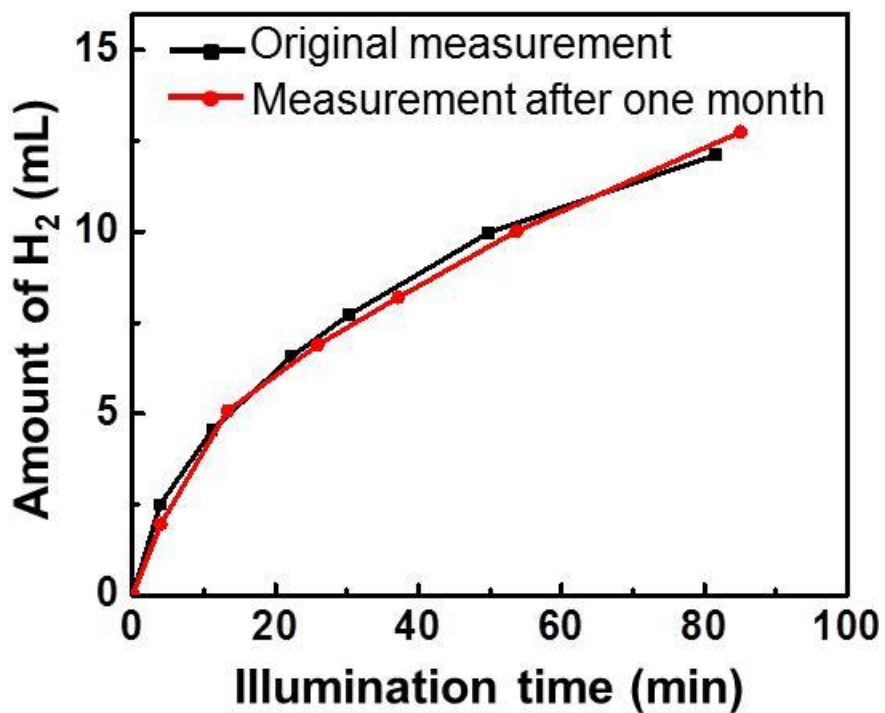


Figure S13. H₂ production ability of 3D Pt-TiO₂ fibrous photocatalyst in capillary design (black curve). After storing the photocatalyst for one month, the H₂ production ability was measured again and shown in red curve.

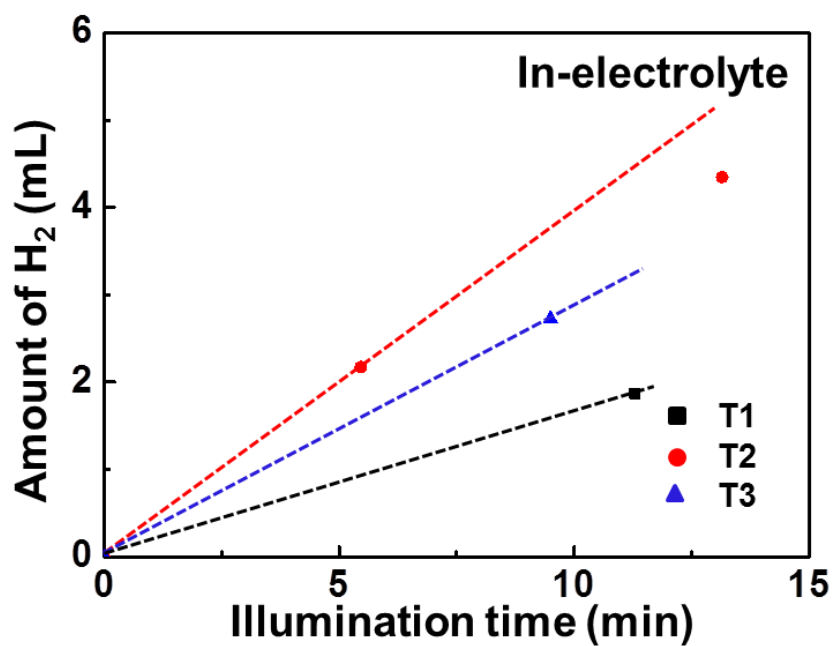


Figure S14. Magnified H₂ evolution curves in in-electrolyte setup of the first 15 min in the presence of T1. Derived initial H₂ production rates were calculated by the indicated dashed lines.

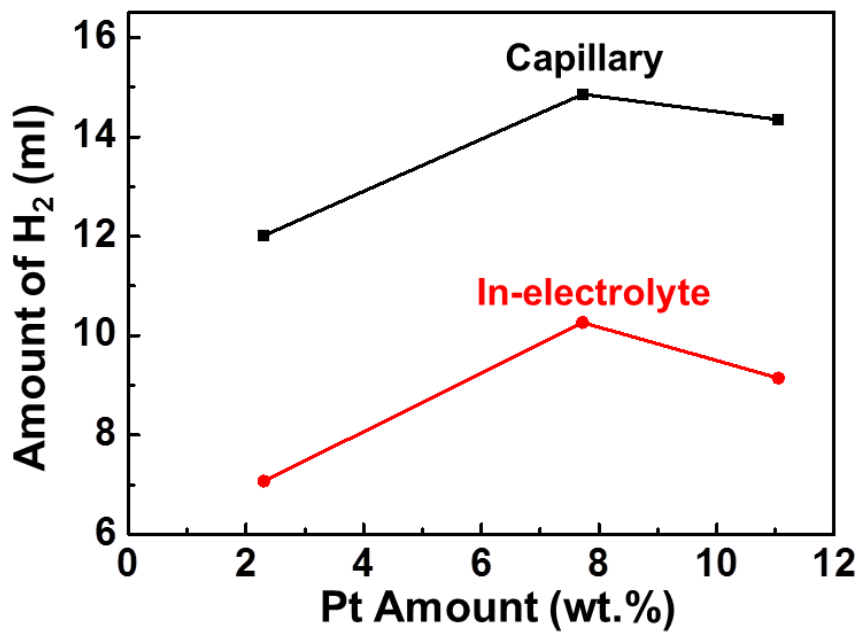


Figure S15. H₂ yield of both capillary and in-electrolyte measurement from three 3D Pt-TiO₂ fibrous structures (T1, T2, and T3) with different Pt contents.